

ORIGINAL ARTICLE

Forensic Age Estimation using CBCT-Derived Mandibular Morphometrics: A Comparative Study of Regression and Machine-Learning Models

Asheerbad Swain¹, Kamala K.A.², Suraiya Khan³, Anish Nelson⁴,
Rahul Tiwari⁵, Heena Dixit Tiwari⁶, Manish Sharma⁷

HOW TO CITE THIS ARTICLE:

Asheerbad Swain, Kamala K.A., Suraiya Khan, et al. Forensic Age Estimation Using CBCT-Derived Mandibular Morphometrics: A Comparative Study of Regression and Machine-Learning Models. Indian J Forensic Med Pathol. 2026; 19(2): 133-144.

ABSTRACT

Background: Accurate age estimation in adolescents and adults remains challenging in forensic practice once dental development is complete. Cone-beam computed tomography (CBCT) enables three-dimensional evaluation of skeletal structures and may improve age estimation without additional radiation exposure.

Aim: To develop and internally validate a CBCT-based multivariate regression model for chronological age estimation using mandibular morphometrics and to compare its performance with a machine-learning approach.

Materials and Methods: This retrospective study analyzed 150 CBCT scans of individuals aged 10–70 years. Mandibles were segmented using ITK-SNAP software, and standardized three-dimensional morphometric measurements were obtained. The dataset was randomly divided into a training set (n = 105) and a

AUTHOR'S AFFILIATION:

¹ Postgraduate Student, Department of Public Health Dentistry, Kalinga Institute of Dental Sciences, Kalinga Institute of Industrial Technology (Deemed to be University), Bhubaneswar, Odisha, India.

² Associate Professor, Department of Oral Medicine and Radiology, School of Dental Sciences, Krishna Vishwa Vidyapeeth (Deemed to be University), Satara, Maharashtra, India.

³ Department of Public Health, Johns Hopkins Bloomberg School of Public Health, Baltimore, United States.

⁴ Lecturer, Department of Oral and Maxillofacial Surgery, AB Shetty Memorial Institute of Dental Sciences, Nitte (Deemed to be University), Mangalore, India.

⁵ Adjunct Professor, Department of Dental Research Cell, Dr. D. Y. Patil Dental College & Hospital, Dr. D. Y. Patil Vidyapeeth (Deemed to be University), Pimpri, Pune, India.

⁶ Programme Officer, Blood Cell, Commissionerate of Health and Family Welfare, Government of Telangana, Hyderabad, India.

⁷ Professor and Head, Department of Oral and Maxillofacial Pathology, Jawahar Medical Foundation's Annasaheb Chudaman Patil Memorial Dental College, Dhule, Maharashtra, India.

CORRESPONDING AUTHOR:

Kamala K.A. Associate Professor, Department of Oral Medicine and Radiology, School of Dental Sciences, Krishna Vishwa Vidyapeeth (Deemed to be University), Satara, Maharashtra, India.

E-mail: kamsweetsmile@gmail.com

➤ **Received:** 29-12-2025 ➤ **Accepted:** 06-03-2026



Creative Commons Non Commercial CC BY-NC: This article is distributed under the terms of the Creative Commons Attribution NonCommercial 4.0 License (<http://www.creativecommons.org/licenses/by-nc/4.0/>) which permits non-Commercial use, reproduction and distribution of the work without further permission provided the original work is attributed as specified on the Red Flower Publication and Open Access pages (<https://www.rfppl.co.in>)

testing set ($n = 45$). Pearson's correlation analysis and stepwise multivariate linear regression were used to develop the regression model. A Random Forest regression model was trained for comparison. Model performance was assessed using the coefficient of determination (R^2), root mean square error (RMSE), mean absolute error (MAE), and mean absolute percentage error (MAPE). Agreement between predicted and chronological age was evaluated using Bland-Altman analysis and intraclass correlation coefficient (ICC).

Results: Chronological age showed a strong positive correlation with the gonial angle and a strong negative correlation with the ramus height-to-body length ratio. The final regression model retained gonial angle, bicondylar width, and ramus height-to-body length ratio as significant predictors. In the testing dataset, the regression model demonstrated excellent predictive accuracy ($R^2 = 0.881$; RMSE = 6.09 years; MAE = 5.89 years), minimal bias (-0.49 years), and excellent agreement (ICC = 0.90). The Random Forest model showed reasonable performance but did not outperform the regression model.

Conclusion: CBCT-derived mandibular morphometrics enable accurate, non-invasive forensic age estimation. The regression model demonstrated superior reliability and interpretability compared with machine-learning, supporting its clinical and medico-legal applicability.

Key findings

1. A regression-based model using CBCT-derived mandibular morphometrics achieved high predictive accuracy and agreement for forensic age estimation, outperforming the machine-learning approach in internal validation.
2. Mandibular shape and angular parameters, particularly gonial angle and ramus height-to-body length ratio, were more reliable indicators of chronological age than isolated linear mandibular measurements.

KEYWORDS

• Age • Estimation • Forensic • Mandibular • Morphology

INTRODUCTION

Accurate and reliable estimation of chronological age is essential in forensic anthropology, clinical forensic medicine, orthodontics, paediatric endocrinology, and legal proceedings involving unaccompanied minors or unidentified human remains, particularly when birth records are missing, unreliable, or deliberately falsified.¹ In adolescents and adults, age estimation becomes increasingly challenging once dental development is complete, as most odontogenic indicators lose their discriminatory value. Conventional radiographic approaches such as hand-wrist analysis and cervical vertebral maturation staging remain widely used but are limited by additional radiation exposure, moderate inter-observer reproducibility, and susceptibility to systemic factors including nutrition and hormonal status.²

Cone-beam computed tomography (CBCT) has become an integral imaging modality in orthodontic, maxillofacial, and forensic practice, offering high-resolution three-dimensional visualization of craniofacial structures at radiation doses substantially lower than those of conventional medical CT.³ The mandible, owing to its dense cortical structure, biomechanical loading patterns, and resistance to post-mortem degradation, frequently preserves identifiable morphological characteristics even in advanced decomposition or thermal damage, making it particularly valuable for forensic age estimation.⁴

Previous investigations have explored age-related changes in mandibular morphometrics, including bicondylar width, bigonial width, ramus height, gonial angle, and condylar dimensions, reporting moderate to strong correlations across different

populations.^{5,6} However, many of these studies relied on two-dimensional imaging or isolated linear measurements, which may inadequately capture complex age-related shape remodeling. Geometric morphometric approaches have demonstrated improved discriminatory potential by emphasizing shape rather than size alone. Puspa Larasati *et al.*⁷, using panoramic radiographs, identified significant age-related mandibular shape variations involving the gonial region and ramus, but their methodology was constrained by the inherent limitations of two-dimensional projection.

Despite the growing availability of CBCT datasets in orthodontic and forensic practice, there is still a lack of rigorously validated multivariate models that integrate three-dimensional mandibular morphometric parameters for chronological age estimation across adolescence and adulthood. Furthermore, although machine-learning approaches are increasingly explored in forensic age assessment, direct comparisons with conventional regression-based models, particularly in terms of predictive accuracy, bias, and agreement with chronological age, remain limited. Therefore, the aim of the present study was to develop and internally validate a population-specific, CBCT-based multivariate regression model for chronological age estimation using mandibular morphometrics and to compare its predictive performance with that of a machine-learning model. The specific objectives were (i) to evaluate associations between chronological age and CBCT-derived linear, angular, and ratio-based mandibular parameters, (ii) to derive a parsimonious regression equation using the most significant mandibular predictors, (iii) to assess and compare model performance using error metrics, and (iv) to evaluate agreement between predicted and chronological age using Bland-Altman analysis and intraclass correlation coefficient (ICC), thereby determining the forensic reliability and clinical applicability of CBCT-derived mandibular morphometrics without additional radiation exposure.

MATERIALS AND METHODS

Study design and ethical approval

This retrospective observational study was conducted in August 2025 using cone-beam computed tomography (CBCT) scans

retrieved from the institutional radiology database from January 2019 to July 2025. The study followed the ethical principles outlined in the Declaration of Helsinki, and approval was obtained from the Institutional Ethical Committee prior to data collection. All images were anonymized before analysis to ensure participant confidentiality. Since this study utilized pre-existing radiographic data, the requirement for individual informed consent was waived.

Sample and eligibility criteria

CBCT scans of individuals aged 10–70 years were screened to ensure a broad representation of mandibular morphological variation across adolescence to late adulthood. Only high-quality scans with complete visualization of both mandibular rami and the body were included. Scans showing pathology, fractures, craniofacial syndromes, previous mandibular surgery, or significant artefacts were excluded. A single, continuous sample was obtained without subgroup stratification; all eligible scans were retained to avoid selection bias.

The sample size was determined to obtain stable estimates for a multivariable linear regression model predicting chronological age from mandibular morphometric variables. Based on Green's rule of thumb for multiple regression ($N \geq 50 + 8m$, where m is the number of predictors in the final model)⁸, a minimum of 74 subjects would be required for a model including three predictors. To further enhance precision and allow internal validation, we included a total of 150 CBCT scans, which were randomly split into a training set ($n = 105$) and a testing set ($n = 45$).

A total of 150 eligible CBCT scans were included. The entire dataset was randomly divided into a training set (70%, $n = 105$) for development of the regression model and a testing set (30%, $n = 45$) for independent internal validation. This split-sample approach minimized overfitting and allowed objective evaluation of predictive performance.

CBCT acquisition parameters

All CBCT scans were acquired using a standardized institutional imaging protocol on a single CBCT system. Acquisition parameters ranged within routine diagnostic limits, with a field of view of 12–17 cm, voxel size of 0.2–

0.3 mm, tube voltage of 90–120 kVp, and tube current of 5–10 mA. All scans met diagnostic image quality requirements for three-dimensional morphometric analysis.

Mandibular segmentation and 3D reconstruction

The anonymized Digital Imaging and Communications in Medicine (DICOM) datasets were imported into ITK-SNAP software (version 3.8.0; Penn Image Computing and Science Laboratory, University of Pennsylvania, Philadelphia, PA, USA) for three-dimensional segmentation and analysis using the built-in semi-automated active contour (region-growing) module. The mandible was segmented semi-automatically using a threshold-based active contour region-growing algorithm. An initial global intensity threshold was applied to isolate mineralized structures, following which region growing was restricted to the mandibular compartment. Manual refinement

was subsequently performed in the axial, coronal, and sagittal planes to remove residual maxillary structures, cranial base components, and artefacts, ensuring complete isolation of the mandibular condyles, coronoid processes, rami, body, and symphysis. Segmentation accuracy was visually verified in all three orthogonal planes prior to surface mesh generation.

The segmented volumes were converted into three-dimensional surface renderings. Each mandible was re-oriented so that the Frankfort horizontal plane was aligned parallel to the horizontal axis and the midsagittal plane was perpendicular to it. This standardization minimized positional variability across scans and ensured uniform measurement orientation. Representative examples of the ITK-SNAP-based mandibular segmentation, landmark identification, and morphometric measurements are shown in Figure 1.

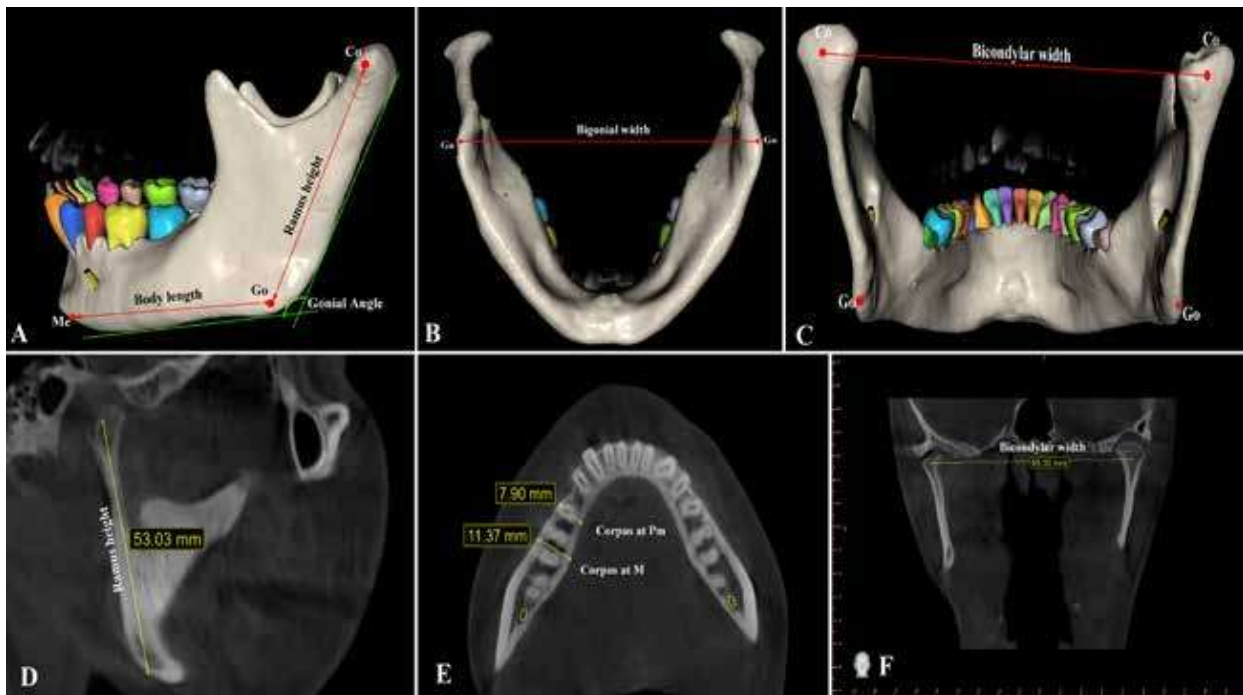


Figure 1: ITK-SNAP-based mandibular segmentation and morphometric measurements derived from cone-beam computed tomography (CBCT); **A:** Three-dimensional mandibular surface model generated following semi-automated segmentation in ITK-SNAP, illustrating landmark identification and linear and angular measurements, including ramus height (Condylion–Gonion), mandibular body length (Menton–Gonion), and gonial angle; **B:** Inferior view of the segmented mandibular surface model showing measurement of bigonial width between bilateral gonion points; **C:** Posterior view of the segmented mandible demonstrating bicondylar width measured between the most superior points of the right and left condyles (Condylion–Condylion); **D:** Sagittal CBCT slice used during ITK-SNAP segmentation depicting linear measurement of ramus height; **E:** Axial CBCT slice illustrating corpus thickness measurements at the premolar (Pm) and molar (M) regions; **F:** Coronal CBCT slice demonstrating bicondylar width measurement in the frontal plane.

Landmark identification

Anatomical landmarks were selected based on reproducibility and previous mandibular morphometric literature. The following landmarks were identified on the 3D surface models:

- Condylion (Co): most superior point on the mandibular condyle
- Gonion (Go): most posterior-inferior point at the mandibular angle
- Menton (Me): most inferior midline point of the mandibular symphysis
- Mandibular notch: deepest point of the sigmoid notch
- Inferior border reference points along the mandibular corpus

All landmarks were placed manually by a calibrated examiner using ITK-SNAP. Cartesian coordinates (x, y, z) of each landmark were exported for morphometric analysis.

Mandibular Morphometric Measurements

A set of linear, angular, and ratio-based morphometric variables was generated from the landmark coordinates. Linear parameters included ramus height, mandibular body length, bicondylar width, bigonial width, condylar width, and corpus thickness at standardized reference points. Angular parameters included gonial angle and mandibular plane angle. Shape-based metrics such as ramus height-body length ratio, and bigonial-bicondylar proportions were derived to minimize variability related to sex or craniofacial size. Bilateral measurements were obtained on both sides and averaged where applicable. Ratios were computed to reduce the influence of absolute craniofacial size and biological sex. The complete definitions of all mandibular variables are provided in Table 1.

Table 1: Definitions of mandibular morphometric variables and derived ratios

Variable	Abbreviation	Definition / Landmark Basis	Side	Unit	Type
Ramus height	RH	Distance from condylion (Co) to gonion (Go)	Right & left (mean)	mm	Linear
Mandibular body length	BL	Distance from gonion (Go) to menton (Me)	Right & left (mean)	mm	Linear
Bicondylar width	BCW	Distance between right and left condylion (Co-Co)	Bilateral	mm	Linear
Bigonial width	BGW	Distance between right and left gonion (Go-Go)	Bilateral	mm	Linear
Condylar width	CW	Maximum mediolateral width of mandibular condyle	Right & left (mean)	mm	Linear
Corpus thickness at first premolar region	CTPM	Buccolingual thickness at first premolar level	Single	mm	Linear
Corpus thickness at first molar region	CTM	Buccolingual thickness at first molar level	Single	mm	Linear
Gonial angle	GA	Angle between ramus plane and mandibular body plane	Right & left (mean)	°	Angular
Mandibular plane angle	MPA	Angle between mandibular plane and Frankfort plane	Global	°	Angular
Ramus height-to-body length ratio	RH/BL	Mean RH ÷ mean BL	Global	Unitless	Ratio
Bigonial-to-bicondylar ratio	BGW/BCW	BGW ÷ BCW	Global	Unitless	Ratio

Values are measured on standardized 3D CBCT reconstructions using ITK-SNAP software.

Observer reliability assessment

To assess intra- and inter-observer reliability, 20 CBCT scans were randomly selected and re-measured after a two-week interval. Measurements were repeated by the primary examiner and independently by a second examiner using the same ITK-SNAP workflow.

Intraclass correlation coefficients (ICC) were calculated using a two-way random-effects model with absolute agreement for single measures. An ICC ≥ 0.80 was considered indicative of acceptable reliability. Measurements with poor reproducibility were excluded from subsequent analysis. The mandibular morphometric measurements

demonstrated good to excellent intra- and inter-observer reliability (ICC \geq 0.80), supporting the robustness of the landmarking and measurement protocol.

Statistical analysis and regression model development

Descriptive statistics, including means, standard deviations, and 95% confidence intervals, were calculated for chronological age and all mandibular morphometric variables in both the training and testing datasets. In the training dataset, Pearson's correlation analysis was performed to examine associations between chronological age and individual mandibular parameters.

Variables demonstrating statistically significant correlations and/or strong biological plausibility were entered into a stepwise multivariate linear regression model, with chronological age (in years) as the dependent variable. The stepwise selection procedure was used to identify the most parsimonious combination of predictors contributing to age estimation. Multicollinearity among independent variables was assessed using variance inflation factors (VIF), with values below 5 considered acceptable. Regression coefficients, standard errors, and confidence intervals were calculated, and the final regression equation was derived from the training dataset.

Model validation and comparative analysis

The derived regression equation was applied to the independent testing dataset for internal validation. Predictive performance was evaluated in both the training and testing datasets using the coefficient of determination (R^2), root mean square error (RMSE), mean absolute error (MAE), and mean absolute percentage error (MAPE).

For comparative analysis, a machine-learning model based on the Random Forest regression algorithm was developed using the same training dataset. Random Forest was selected due to its ability to model complex non-linear relationships and reduce overfitting through ensemble learning. The model was trained using default hyperparameters, with multiple decision trees generated from bootstrapped samples of the training data and random subsets of predictors selected at each split. The trained Random Forest model

was then applied to the independent testing dataset. Predictive performance metrics for the regression-based and Random Forest models were calculated using identical criteria to allow direct comparison of accuracy and generalizability.

Agreement analysis

Agreement between predicted age and actual chronological age was assessed using Bland-Altman analysis. Mean difference (bias) and 95% limits of agreement were calculated to evaluate systematic bias and dispersion between predicted and observed values for both the regression and Random Forest models.

Additionally, intraclass correlation coefficient (ICC) analysis was performed to quantify the degree of agreement between predicted and actual age values. A two-way random-effects model with absolute agreement was used, and ICC values were interpreted according to established reliability thresholds.

Data management and reporting standards

All cases were analyzed according to a pre-registered protocol based on established radiomorphometric and CBCT reporting guidelines. Data handling followed STROBE recommendations for observational research. Reporting of findings was aligned with forensic age-estimation best-practice statements to ensure clinical applicability.

RESULTS

The cohorts are closely matched in age (40.14 ± 15.48 vs. 39.21 ± 16.93 years) and across all measured mandibular dimensions. Key anatomical means, such as bicondylar width (117.54 ± 10.10 mm vs. 115.69 ± 8.15 mm) and bigonial width (93.50 ± 7.99 mm vs. 94.02 ± 8.78 mm), show negligible variation. Slightly greater divergence was noted in angular measurements, particularly the gonial angle ($122.23 \pm 5.56^\circ$ vs. $124.63 \pm 6.27^\circ$) and mandibular plane angle ($27.25 \pm 4.74^\circ$ vs. $28.83 \pm 5.56^\circ$). Crucially, the derived ratios for ramus-to-body and bigonial-to-bicondylar proportions were nearly identical. This close alignment infers that the testing sample is demographically and morphologically representative of the training population. Therefore, the testing dataset is validated as a suitable and reliable subset for externally evaluating any predictive models

developed from the training data, minimizing the risk of bias due to sample stratification (Table 2).

Table 2: Descriptive statistics of demographic and mandibular morphometric variables in training and testing datasets

Variables	Unit	Training data (n=105)	Mean at 95% Confidence Interval		Testing data (n=45)	Mean at 95% CI	
		Mean ± SD	Lower limit	Upper limit	Mean ± SD	Lower limit	Upper limit
Age	Years	40.14 ± 15.48	37.141	43.131	39.21 ± 16.93	34.12	44.29
Ramus height	mm	53.75 ± 5.53	52.683	54.824	55.09 ± 5.21	53.53	56.66
Mandibular body length	mm	78.33 ± 7.36	76.904	79.753	78.98 ± 7.34	76.77	81.18
Bicondylar width	mm	117.54 ± 10.10	115.588	119.499	115.69 ± 8.15	113.24	118.14
Bigonial width	mm	93.50 ± 7.99	91.956	95.048	94.02 ± 8.78	91.38	96.65
Condylar width	mm	19.45 ± 1.75	19.108	19.787	19.41 ± 1.92	18.83	19.98
Corpus thickness at premolar region	mm	10.92 ± 1.39	10.653	11.193	11.24 ± 1.44	10.8	11.67
Corpus thickness at molar region	mm	12.43 ± 1.64	12.114	12.748	12.21 ± 1.72	11.7	12.73
Gonial angle	Degrees	122.23 ± 5.56	121.155	123.306	124.63 ± 6.27	122.74	126.51
Mandibular plane angle	Degrees	27.25 ± 4.74	26.332	28.167	28.83 ± 5.56	27.16	30.5
Ramus height-to-body length	Ratio	0.69 ± 0.09	0.674	0.71	0.7 ± 0.1	0.67	0.73
Bigonial width-to-bicondylar width	Ratio	0.80 ± 0.09	0.783	0.819	0.82 ± 0.09	0.79	0.84

Values are presented as mean ± standard deviation (SD) with 95% confidence intervals (CI).

The correlation analysis revealed that, within the training sample, chronological age showed significant correlations with specific mandibular dimensions. A strong positive correlation was found with the gonial angle ($r=0.722$, $p=0.001$), indicating this angle increases markedly with age. Conversely, significant negative correlations were observed

for bicondylar width ($r=-0.369$, $p=0.001$) and, most strongly, for the ramus width-to-body length ratio ($r=-0.792$, $p=0.001$). Corpus thickness at the molar region also showed a weak positive correlation ($r=0.242$, $p=0.021$). All other variables, including most linear measurements, demonstrated no statistically significant relationship with age (Table 3).

Table 3: Correlation between mandibular variables (training data) and chronological age

Variables	Chronological age (years)	
	r value	p-value
Ramus height (mm)	-0.015	0.881
Mandibular body length (mm)	0.123	0.211
Bicondylar width (mm)	-0.369	0.001*
Bigonial width (mm)	0.075	0.45
Condylar width (mm)	-0.033	0.739
Corpus thickness at premolar region (mm)	-0.005	0.958
Corpus thickness at molar region (mm)	0.242	0.021*
Gonial angle (degrees)	0.722	0.001*
Mandibular plane angle (degrees)	0.041	0.681
Ramus height-to-body length ratio	-0.792	0.001*
Bigonial width-to-bicondylar width ratio	-0.006	0.956

r = Pearson correlation coefficient., Correlation strength was interpreted as negligible ($|r| < 0.20$), weak (0.20-0.39), moderate (0.40-0.59), strong (0.60-0.79), and very strong (≥ 0.80).

*p < 0.05 indicates statistical significance.

The stepwise regression analysis produced two significant models for predicting age using mandibular variables. The final and most parsimonious model (Model 2) retained three key predictors: Bicondylar width, gonial angle, and the ramus width-to-body length ratio, all with high statistical significance (p=0.001). This inference strongly confirms that specific mandibular proportions are reliable

indicators of chronological age. The exclusion of other variables, such as corpus thickness at molar region, through the stepwise process indicates that the three retained measurements provide a statistically sufficient and powerful combination for age estimation, highlighting their utility in anatomical and forensic applications (Table 4).

Table 4: Multivariate linear regression model (stepwise) applied to training data

Model 1	B	Standard Error	T stats	p-value	CI at 95% (lower limit)	CI at 95% (upper limit)
Constant	32.29	20.70	1.56	0.122	-8.31	72.89
Bicondylar width	-0.29	0.06	-4.51	0.001*	-0.41	-0.17
Corpus thickness at molar region	0.73	0.47	1.53	0.128	-0.19	1.65
Gonial angle	0.61	0.11	5.40	0.001*	0.39	0.83
Ramus height-to-body length ratio	-60.81	7.97	-7.63	0.001*	-76.43	-45.19
Model 2						
Constant	43.74	19.43	2.25	0.026	5.66	81.82
Bicondylar width	-0.30	0.06	-4.66	0.001*	-0.42	-0.18
Gonial angle	0.61	0.11	5.35	0.001*	0.39	0.83
Ramus height-to-body length ratio	-62.81	7.95	-7.84	0.001*	-78.39	-47.23

B = unstandardized regression coefficient; CI = confidence interval. *p < 0.05 indicates statistical significance.

The regression equation thus formed is shown in Table 5. Table 6 summarizes the predictive performance of the regression equation and machine-learning model across training and testing datasets. The regression model demonstrated good accuracy with lower error metrics and higher explained variance in both datasets, indicating stable predictive performance. The machine-learning model showed comparatively higher error values and lower R², particularly in the testing dataset, suggesting reduced generalizability when compared with the regression approach.

Table 5: Regression equation

Final age prediction equation
Age (years) = 43.74 - (0.30 × Bicondylar width [mm]) + (0.61 × Gonial angle [°]) - (62.81 × Ramus height-to-body length ratio)

Table 6: Regression model validation and performance metrics

	Training data (n=105)	Testing data (n=45)	Machine model
RMSE	7.81	6.09	8.75
MAE / MAD	5.58	5.89	7.72
MAPE	16.05%	22.23%	19.2%
R ²	0.752	0.881	0.674

RMSE = root mean square error; MAE = mean absolute error; MAPE = mean absolute percentage error; R² = coefficient of determination.

Table 7 presents the Bland-Altman agreement analysis between chronological age and predicted age. The regression equation showed a smaller mean difference (bias) and narrower limits of agreement, reflecting closer agreement with actual chronological age. In contrast, the machine-learning model exhibited a higher bias and wider limits of agreement, indicating greater variability in age prediction.

Table 7: Bland-Altman analysis showing agreement between chronological age and age predicted using regression equation and machine-learning model

Parameter	Equation	Machine model
Mean difference (bias)	-0.49	0.371
Upper limit of agreement	3.35	6.46
Lower limit of agreement	-5.32	-7.75

Table 8 shows the intraclass correlation coefficient (ICC) analysis for agreement between predicted and actual chronological age. Both models demonstrated excellent agreement, with ICC values above 0.85 and statistically significant results (p = 0.001). However, the regression equation achieved a slightly higher ICC than the machine-learning model, further supporting its superior reliability in age prediction.

Table 8: Intraclass correlation coefficient (ICC) analysis demonstrating agreement between predicted and actual chronological age for regression and machine-learning models

Intraclass correlation coefficient	ICC	Lower 95%-CI	Upper 95%-CI	F stats	p-value
Regression equation	0.90	0.83	0.94	18.83	0.001
Machine model	0.88	0.83	0.92	18.12	0.001

P < 0.05: statistically significant

DISCUSSION

Accurate estimation of chronological age in adolescents and adults remains a major challenge in forensic sciences because most dental development-based methods lose discriminatory power after completion of tooth mineralization.⁹ Consequently, skeletal approaches assume greater importance in this age group, particularly in scenarios involving fragmentary remains or undocumented individuals. Among skeletal elements, the mandible is especially valuable for forensic identification and age estimation owing to its dense cortical structure, resistance to post-mortem degradation, and sustained exposure to functional and biomechanical remodeling throughout life.⁴ The present study reinforces this premise by demonstrating that three-dimensional CBCT-derived mandibular morphometrics can be integrated into a robust multivariate regression model with excellent predictive accuracy, thereby overcoming key limitations associated with two-dimensional imaging and single-parameter approaches.⁶

One of the most influential findings of the present study is the strong association observed between chronological age and the gonial angle. Age-related changes in the gonial region have been extensively documented in both anthropological and clinical radiology literature.¹⁰ Early panoramic radiographic studies reported progressive widening of the gonial angle with advancing age, attributed to alveolar bone resorption, muscular remodeling, and alterations in occlusal loading patterns.^{11,12} In contrast, Bakan *et al.*¹³, using CBCT images of dentate individuals aged 7–17 years, reported no significant correlation between age and gonial angle. This discrepancy may be explained by differences in age range, population-specific craniofacial morphology, and the limited manifestation of age-related mandibular remodeling in younger individuals. The present findings suggest that gonial angle becomes a more sensitive indicator of age-related change when broader age ranges extending into adulthood are examined.

Equally noteworthy is the identification of the ramus height-to-body length ratio as a superior predictor of chronological age compared with isolated linear mandibular measurements. This observation aligns with geometric morphometric and forensic anthropological evidence indicating that proportional indices more effectively capture age-related shape transformations than absolute dimensions.¹⁴ Puspa Larasati *et al.*⁷, using geometric morphometric analysis on panoramic radiographs, demonstrated significant age-related mandibular shape variation, particularly in the gonial and ramal regions, achieving classification accuracies of 67% in adults and 65% in adolescents. However, their study was constrained by two-dimensional projection errors. By employing three-dimensional CBCT data, the present study extends these findings and confirms that mandibular shape ratios retain strong biological relevance even when absolute mandibular size exhibits weak age dependence.

The inclusion of bicondylar width in the final regression model is also consistent with existing evidence on condylar remodeling. The mandibular condyle is highly responsive to masticatory forces, adaptive remodeling of the temporomandibular joint, and age-related degenerative changes.¹⁵ Uzel *et al.*¹⁶ demonstrated the utility of CBCT-based radiomic analysis of the mandibular condyle for age estimation, while Valladares Neto *et al.*¹⁷ reported age-related increases primarily in the frontal dimension of the condyle in individuals aged 3–20 years. The present study corroborates these observations and indicates that bicondylar width contributes meaningful discriminatory information when combined with angular and proportional mandibular variables.

In contrast, most isolated linear mandibular dimensions, including ramus height and mandibular body length, exhibited weak independent associations with age. This finding supports previous work by Singh *et al.*¹⁸, who reported strong sexual dimorphism but limited

age dependence for individual mandibular dimensions in adults. These observations help explain the modest performance of earlier linear-only mandibular age estimation models and underscore the importance of multivariate frameworks that integrate size, shape, and angular parameters.

The predictive accuracy achieved in the present study compares favorably with previously reported adult age estimation methods. Dental-based CBCT approaches, such as pulp-tooth ratio analysis, typically report mean absolute errors ranging from ± 7 to ± 12 years.^{19,20} Artificial intelligence-based dental age estimation methods have demonstrated moderate correlations with chronological age ($r = 0.65$, $p < 0.001$) and a mean absolute error of approximately 4.7 years²¹, while deep learning approaches using orthopantomograms have reported prediction accuracies of around 63% within one year of actual age.²² In comparison, the CBCT-based mandibular regression model developed in the present study demonstrated lower error margins and stronger agreement with chronological age. Although the Random Forest machine-learning model incorporated in this study was able to model non-linear relationships and achieved reasonable predictive performance, it did not outperform the regression-based approach in terms of accuracy or agreement. This finding suggests that, in anatomically interpretable datasets with well-defined morphometric predictors, parsimonious regression models may offer superior generalizability and forensic transparency compared with more complex machine-learning algorithms.

From a methodological perspective, this study offers several strengths. First, CBCT imaging eliminates magnification and superimposition errors inherent to panoramic radiography, enabling true three-dimensional spatial assessment. Second, the use of standardized ITK-SNAP-based segmentation and reorientation protocols resulted in high intra and inter-observer reliability, consistent with prior validations of ITK-SNAP in craniofacial morphometric research.^{22,23} Third, the adoption of a split-sample internal validation strategy enhanced the statistical rigor of the analysis and reduced the risk of overfitting, thereby strengthening the credibility and reproducibility of the proposed regression model.

Clinical and forensic implications

The findings of this study have important clinical and forensic implications. In forensic contexts, the CBCT-based mandibular regression equation may be applied to living age estimation in undocumented individuals, asylum seekers, and legal age disputes, as well as to post-mortem identification in cases involving decomposed, skeletonized, or thermally altered remains. Given that the mandible frequently survives extreme environmental conditions and is often recoverable even when teeth or long bones are unavailable, this approach is particularly valuable in mass disaster and criminal investigation settings.

From a clinical perspective, the method enables opportunistic forensic inference using CBCT scans already acquired for orthodontic, implant, or maxillofacial diagnostic purposes, without additional radiation exposure. The reliance on only three robust and anatomically interpretable mandibular parameters further facilitates practical implementation in routine forensic and medico-legal workflows.

Limitations and future directions

Several limitations should be acknowledged. First, the regression model is population-specific, and variations in craniofacial morphology across ethnic groups may influence predictive accuracy; external validation in diverse populations is therefore essential. Second, although a wide age range was included, uneven age distribution across decades may affect predictive performance at the extremes of age. Third, the analysis was restricted to mandibular variables; future studies integrating maxillary, cervical vertebral, or dental pulp parameters may further enhance accuracy. Finally, while semi-automated segmentation demonstrated excellent reliability, future incorporation of fully automated artificial intelligence-based landmarking and segmentation could improve efficiency and scalability in high-throughput forensic applications.

CONCLUSIONS

This study developed and internally validated a population-specific multivariate regression model for chronological age estimation using CBCT-derived mandibular morphometric parameters. The gonial angle, ramus height-

to-body length ratio, and bicondylar width emerged as the most influential predictors of age, underscoring the importance of mandibular shape and angular remodeling over isolated linear measurements. By utilizing routinely acquired CBCT data, the proposed approach enables accurate and non-invasive age estimation in both living individuals and skeletal remains without additional radiation exposure. The regression model demonstrated strong predictive performance and agreement, offering a scientifically robust and clinically applicable adjunct for contemporary forensic odontology and medico-legal age assessment.

Acknowledgements: None

Funding information: None

Conflict of interest statement: The authors have no conflicts of interest to declare.

Data availability statement: The data that support the findings of this study are available from the corresponding author upon reasonable request.

REFERENCES

1. Ubelaker D.H., Khosrowshahi H. Estimation of age in forensic anthropology: historical perspective and recent methodological advances. *Forensic Sci Res.* 2019; 4(1): 1-9. doi: 10.1080/20961790.2018.1549711.
2. Gabriel D.B., Southard K.A., Qian F, Marshall S.D., Franciscus R.G., Southard T.E. Cervical vertebrae maturation method: poor reproducibility. *Am J Orthod Dentofacial Orthop.* 2009; 136(4): 478.e1-7; discussion 478-80. doi: 10.1016/j.ajodo.2007.08.028.
3. Venkatesh E., Elluru S.V. Cone beam computed tomography: basics and applications in dentistry. *J Istanbul Univ Fac Dent.* 2017; 51(3 Suppl 1): S102-S121. doi: 10.17096/jiufd.00289.
4. Motawei S.M., Helaly A.M., Aboelmaaty W.M., Elmahdy K., Shabka O.A., Liu H. Length of the ramus of the mandible as an indicator of chronological age and sex: a study in a group of Egyptians. *Forensic Sci Int.* 2020; 2 doi: 10.1016/j.fsir.2020.100066.
5. Dogan M.E., Turkoglu B.N., Şengul I. A Morphometric Evaluation of the Mandibular Condyle, Coronoid Process, and Gonial Angle: Age and Gender Differences in CBCT Imaging. *Diagnostics (Basel).* 2025; 15(12): 1459. doi: 10.3390/diagnostics15121459.
6. Arthanari A., Senthilkumar A., Ramalingam K., Prathap L., Ravindran V. Exploring Age and Gender Identification Through Mandibular Parameters Using Orthopantomography: An Observational Study. *Cureus.* 2024; 16(3): e55788. doi: 10.7759/cureus.55788.
7. Puspa Larasati L.D., Kurniawan A., Chusida A., Rizky B.N., Marini M.I., Arisa Putri Q.O., et al. Geometric morphometric analysis of mandibular morphology for age classification in Indonesian adolescents and adults. *J Oral Biol Craniofac Res.* 2025; 15(6): 1518-1525. doi: 10.1016/j.jobcr.2025.09.011.
8. Green S.B. How many subjects does it take to do a regression analysis. *Multivariate Behav Res.* 1991; 26(3): 499-510. doi: 10.1207/s15327906mbr2603_7
9. Vila-Blanco N., Varas-Quintana P., Tomás I., Carreira M.J. A systematic overview of dental methods for age assessment in living individuals: from traditional to artificial intelligence-based approaches. *Int J Legal Med.* 2023; 137(4): 1117-1146. doi: 10.1007/s00414-023-02960-z.
10. IZARD G. The gonio-mandibular angle in dento-facial orthopedia. *Int J Orthodontia.* 1927; 13: 578. doi: 10.1016/S0099-6963(27)90110-0
11. Ohm E., Silness J. Size of the mandibular jaw angle related to age, tooth retention and gender. *J Oral Rehabil.* 1999; 26(11): 883-91. doi: 10.1046/j.1365-2842.1999.00464.x.
12. Leversha J., McKeough G., Myrteza A, Skjellrup-Wakefiled H., Welsh J., Sholapurkar A. Age and gender correlation of gonial angle, ramus height and bigonial width in dentate subjects in a dental school in Far North Queensland. *J Clin Exp Dent.* 2016; 8(1): e49-54. doi: 10.4317/jced.52683.
13. Bakan A., Kervancıoğlu P., Bahşi İ., Yalçın E.D. Comparison of the Gonial Angle With Age and Gender Using Cone-Beam Computed Tomography Images. *Cureus.* 2022; 14(5): e24997. doi: 10.7759/cureus.24997.
14. Mitteroecker P., Schaefer K. Thirty years of geometric morphometrics: Achievements, challenges, and the ongoing quest for biological meaningfulness. *Am J Biol Anthropol.* 2022; 178 Suppl 74(Suppl 74): 181-210. doi: 10.1002/ajpa.24531.
15. Al-Ghurabi Z.H., Al-Bahrani Z.M. Cone Beam Computed Tomography Evaluation of the Morphological Variation and Width in Mandibular Condyle. *J Craniofac Surg.* 2021; 32(5): e479-e481. doi: 10.1097/SCS.00000000000007465.
16. Üzel A., Kuran A., Baysal O., Seki U., Sinanoglu E.A. Age estimation by radiomics analysis of mandibular condylar cone beam computed

- tomography images. *Leg Med (Tokyo)*. 2025; 72: 102560. doi: 10.1016/j.legalmed.2024.102560.
17. Valladares Neto J., Estrela C., Bueno M.R., Guedes O.A., Porto O.C.L., Pécora J.D. Mandibular condyle dimensional changes in subjects from 3 to 20 years of age using Cone-Beam Computed Tomography: A preliminary study. *Dental Press J Orthod*. 2010; 15: 172-81. <https://www.scielo.br/j/dpjo/a/XzKjjZxRLmvnxWDTpnKG5fj/?format=pdf&lang=en>
 18. Singh R., Singh H., Aggarwal N., Sehgal G., Chandel S., Kumar N. Sexual Dimorphism in Mandibular Ramus Morphometry: A Population-Specific Analysis Using Orthopantomograms in the Lucknow Region. *Cureus*. 2025; 17(3): e80515. doi: 10.7759/cureus.80515.
 19. Kvaal S.I., Kolltveit K.M., Thomsen I.O., Solheim T. Age estimation of adults from dental radiographs. *Forensic Sci Int*. 1995; 74(3): 175-85. doi: 10.1016/0379-0738(95)01760-g.
 20. Cameriere R., Ferrante L., Cingolani M. Variations in pulp/tooth area ratio as an indicator of age: a preliminary study. *J Forensic Sci*. 2004; 49(2): 317-9. <https://pubmed.ncbi.nlm.nih.gov/15027553/>
 21. Vodanovic M., Sribar A., Tomljenovic F., Milosevic D., Subasic M. Age Estimation Based On Orthopantomograms Using Artificial Intelligence. *Int Dent J*. 2025; 75: 104186. 10.1016/j.identj.2025.104186
 22. Yushkevich P.A., Piven J., Hazlett H.C., Smith R.G., Ho S., Gee J.C., Gerig G. User-guided 3D active contour segmentation of anatomical structures: significantly improved efficiency and reliability. *Neuroimage*. 2006; 31(3): 1116-28. doi: 10.1016/j.neuroimage.2006.01.015.
 23. Yushkevich P.A., Yang Gao, Gerig G. ITK-SNAP: An interactive tool for semi-automatic segmentation of multi-modality biomedical images. *Annu Int Conf IEEE Eng Med Biol Soc*. 2016; 2016: 3342-3345. doi: 10.1109/EMBC.2016.7591443.